A Nonvolatile Spintronic Memory Element with a Continuum of Resistance States

*Yeyu Fang, R. K. Dumas, T. N. Anh Nguyen, S. M. Mohseni, S. Chung, C. W. Miller, and Johan Åkerman**

A continuum of stable remanent resistance states is reported in perpendicularly magnetized pseudo spin valves with a graded anisotropy free layer. The resistance states can be systematically set by an externally applied magnetic field. The gradual reversal of the free layer with applied field and the field-independent fixed layer leads to a range of stable and reproducible remanent resistance values, as determined by the giant magnetoresistance of the device. An analysis of first-order reversal curves combined with magnetic force microscopy shows that the origin of the effect is the field-dependent population of up and down domains in the free layer.

1. Introduction

Conventional digital magnetic memory devices rely on the realization of two stable magnetic states to encode information.[1] To meet the perpetual demand for increased storage capacity, most approaches aim to increase memory density by reducing the size of the individual memory cells. An alternative scheme is to increase the number of magnetic states allowed by each memory cell. Magnetics-based multi-state memory devices operable at room temperature have been demonstrated using, for example, dipolar effects in magnetic nanowire arrays,[2] Hall effects in systems with fourfold anisotropy,[3,4] and magnetoresistance effects in pseudo spin valves (PSVs).[5–8] For the latter variety, the memory states are generally defined by the relative orientation of magnetization vectors in the various magnetic layers, and they may use complicated structures with multiple free and fixed layers with distinct coercive fields, either with in-plane[9] or perpendicular magnetic anisotropy,[10] all of which complicates the read and write processes. Despite the added complexity, these PSVs are limited to four states. To extend multi-state digital memories well beyond four or eight states,[11] one may instead design entirely analog memories in which the state of a resistive device can be tuned continuously, leading to an infinite number of states. This was recently suggested by Klein et al., whose approach using $L1_0$-FePt based PSVs[12] demonstrated ten distinct levels, with each state defined by the remanent coupling between layers. Unfortunately, achieving $L1_0$-ordered FePt requires high temperatures, which can be technologically problematic. In this work, we demonstrate a room temperature, nonvolatile, memory element with a continuum of resistive states realized in PSVs with perpendicular anisotropy. The remanent resistance states of the free layer are set with a temporarily applied field, and read out by the giant magnetoresistance (GMR) of the PSV. The mechanism underlying this device is the unique field tunability of the free layer domain state (i.e., the relative population of up and down domains), coupled with the stability of that state upon removal of the field. The potential impact of this device structure is underscored by the combination of continuous tunability, state stability, scalability, reproducibility, and fabrication simplicity.

Y. Fang, Dr. R. K. Dumas, Prof. J. Åkerman
Department of Physics
University of Gothenburg
412 96 Gothenburg, Sweden
E-mail: johan.akerman@physics.gu.se
fangyeyu84@gmail.com
Dr. T. N. A. Nguyen, S. M. Mohseni, Dr. S. Chung,
Prof. J. Åkerman
Materials Physics
School of Information and Communication Technology
KTH - Royal Institute of Technology
Electrum 229, 164 40 Stockholm-Kista, Sweden
Prof. C. W. Miller
Department of Physics
University of South Florida
Tampa, FL 33620, USA

DOI: 10.1002/adfm.201202319

2. Results and Discussion

2.1. Thin Film Fabrication

Thin film multilayers with perpendicular magnetic anisotropy have their easy magnetic axis out of the plane. Although counteracted by the in-plane shape anisotropy associated with a thin film, PMA is well established and has been demonstrated in multilayers of Co/Pd, Co/Pt, Ni/Co.[13–15] Our devices use Co/Pd for both the fixed and free layers, separated by a 6-nm Cu interlayer (**Figure 1**a). While our fixed layer is a traditional PMA heterostructure $[Co(0.25)/Pd(0.6)]_{10}Co(0.25)$ (thicknesses are in nm), the free layer heterostructure $[Co([0.2:0.1:1.1])/Pd(0.6)]_{10}$ has a graded perpendicular anisotropy.[16] The notation Co([0.2:0.1:1.1]) indicates that the Co thickness in the free layer is incremented by 0.1 nm for successive repeats of the Co/Pd unit cell. All samples were deposited at room temperature on Si (001) substrates by dc magnetron sputtering in a system with base pressure better than 5×10^{-8} Torr. A Ta(5)/Ru(10)/

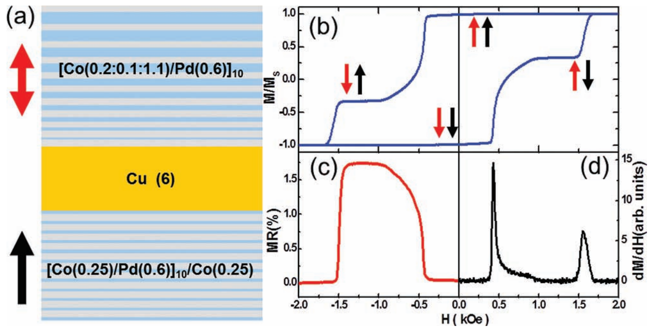

Figure 1. a) Schematic of the device structure showing the graded anisotropy free layer on top separated from the fixed layer on bottom by a Cu spacer (all units are nm). b) Major hysteresis loop of the structure, with the parallel and antiparallel states noted. c) Current-in-plane magnetoresistance of the device with high and low values corresponding to the antiparallel and parallel states. d) Switching field distribution of the device. For (c) and (d), one polarity is shown for brevity; the behavior is symmetric in field.

Ta(5)/Pd(3) seed stack was used to provide a low surface roughness and promote strong PMA in the fixed layer.

2.2. General Device Characterization

Figure 1b shows the 300 K hysteresis loop of the PSV as measured by an alternating gradient magnetometer (AGM). The switching field distribution (SFD; Figure 1d) indicates that the free layer magnetization reversal begins abruptly at –0.39 kOe and becomes fully reversed by –1.05 kOe. The reversal mechanism is the expansion of reverse domains, which proceeds gradually with field due to the perpendicular anisotropy gradient.[16] The fixed layer has a symmetrical SFD that extends from –1.43 to –1.70 kOe. The distinct reversal field ranges for the free and fixed layers enables well defined parallel and antiparallel states. Figure 1c shows that the resultant 300 K current-in-plane magnetoresistance (MR) of the PSV agrees well with the AGM results.

2.3. Novel Observations

The broad SFD of the free layer magnetization enables the PSV magnetoresistance to be set by the partial reversal of the free layer. After saturating the sample, the free layer may be partially reversed by applying a reversal field H_R that lies within the SFD (–1.05 kOe < H_R < –0.39 kOe), then reducing the field to zero. **Figure 2**a shows that the resistance of the PSV depends precisely on the choice of H_R. After removing the field, the relative change in resistance, $(R(H_R)–R(0))/R(H_R)$, is bounded by approximately 0.025%. This suggests that the domain state in the free layer relaxes only slightly upon removal of the field. To demonstrate the stability of the resistance states, we monitored the 300 K resistance for 100 min in zero field, after saturating to 3 kOe, setting each state by distinct H_R, then removing the field. As seen in Figure 2c, each selected state had a constant resistance; the observed fluctuations are on the order of 0.5 mΩ, and are likely due to temperature fluctuations (samples were open

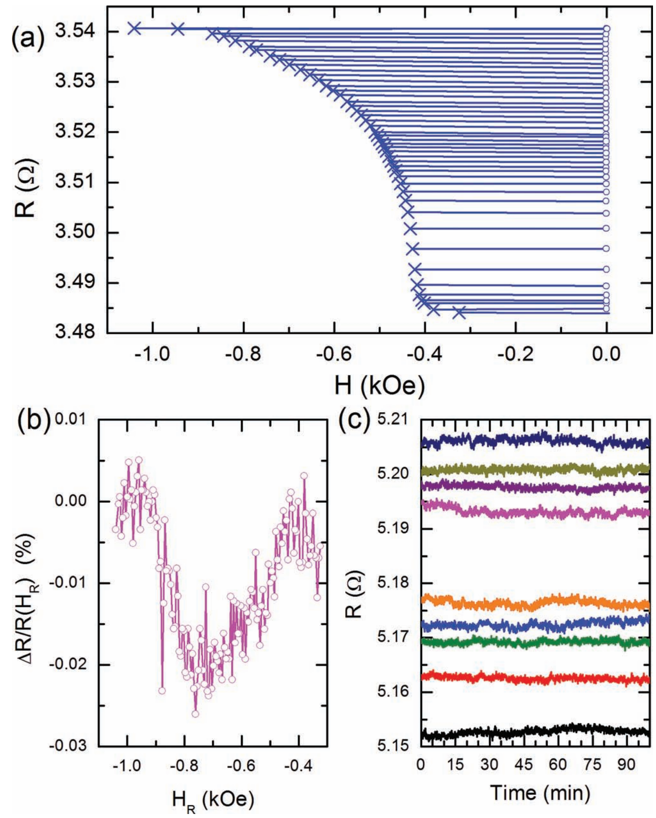

Figure 2. a) The remanent resistance state can be tuned by partially reversing the free layer. The crosses and open circles show the resistance measured at H_R and remanence, respectively. b) The relative resistance change upon removal of the field is on the order of 0.025%. c) The resistance states are essentially independent of time once written by applying H_R after saturation.

to air during these measurements). The states are erased by saturating the PSV in a large magnetic field. The combination of field programmability with stability of the remanent resistance states implies the potential of these devices for nonvolatile multilevel memory applications.

In order to test the reproducibility of the device, we set and read the final state numerous times for six write fields (H_R) spanning the SFD of the free layer. The test protocol was: 1) erase the state by saturating the sample in +4 kOe, then measure $R_{sat} = R(+4\ \text{kOe})$; 2) write the state by setting the field to H_R, then measure $R(H_R)$; 3) reduce the field to zero, then measure $R(0)$. Using $(R(0)–R_{sat})/R_{sat}$) to quantify reproducibility of the write process, the standard deviations of the resistance state (σ) derived from 100 cycles of this protocol for each H_R were bounded above by 2.8% of the mean value for each state, with values 0.002–0.003% for H_R –0.65 kOe and above (i.e., after the initial nucleation and propagation of reverse domains). This indicates good write reproducibility and, more importantly, allows us to estimate the number of states available. We can conservatively approximate the number of distinct states available in the device by dividing the MR range for the employed H_R by twice the largest observed standard deviation in that range: $N_{states} = [MR(H_{R>})–MR(H_{R<})]/(2\sigma_{max})$. This device can thus accommodate 76 distinct states for –0.95 kOe < H_R < –0.45 kOe, where MR(–0.45 kOe) = 0.14%, MR(–0.95 kOe) = 1.12%, and σ_{max} = 0.0064%. A more liberal estimation sums the available states in smaller field steps and uses the average standard deviation between these fields: $N_{states} = \Sigma_i[MR(H_{R,i})-MR(H_{R,i+1})]/(\sigma_i + \sigma_{i+1})$. Using 0.1 kOe field steps from –0.45 to –0.95 kOe, this method indicates the present device is capable of roughly 132 distinct states. Even with a stringent 6-σ requirement, this device offers 44 unique resistive states.

2.4. Explanation for Observations

2.4.1. First Order Reversal Curves Analysis

To more thoroughly understand the origin of these observations, the magnetic reversal mechanism of the PSV was investigated by an analysis of first order reversal curves (FORCs).[17–20] A single FORC curve is measured by: (a) positively saturating the sample; (b) reducing the applied field to H_R; and (c) measuring the magnetization as H increased from H_R back to positive saturation. As shown in **Figure 3**a, compiling a family of FORCs for different H_R fills the interior of the major hysteresis loop, with the outer boundary of the set corresponding to the major loop (e.g., Figure 1b). From this, we see that the remanent magnetization, M_R, of the free layer has a one-to-one correspondence with H_R. That M_R is slightly different from $M(H_R)$

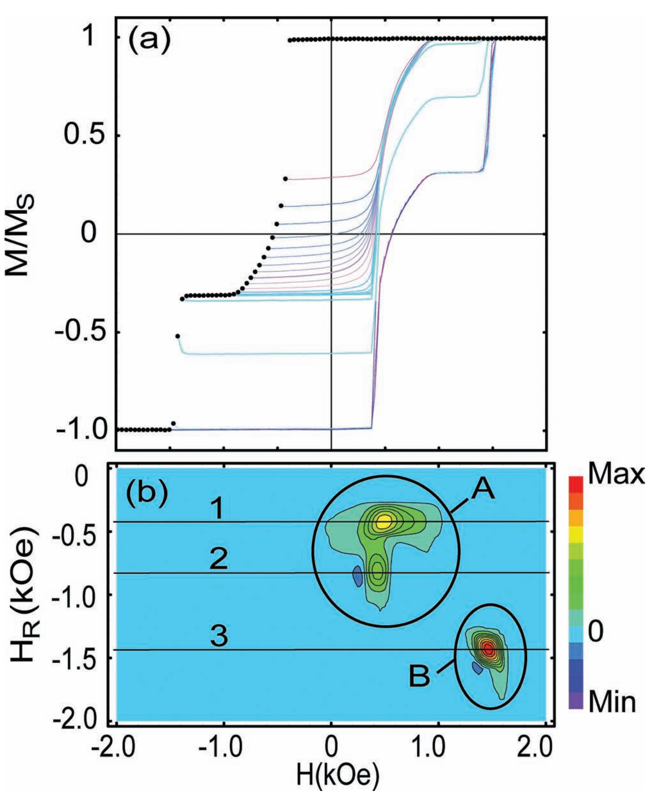

Figure 3. a) Family of FORCs for the PSV, with the first point of the individual reversal curves shown by a black dot. b) The FORC distribution reveals features related to the reversal of the free layer (area A) and fixed layer area (B).

indicates a relaxation of the magnetic domain state toward positive saturation, corroborating the minor relative resistance change with removal of the field (see Figure 2b).

FORC distributions defined by a mixed second-order derivative

$$\rho(H, H_R) \equiv -\frac{1}{2}\frac{\partial^2 M(H, H_R)/M_S}{\partial H \partial H_R}, \quad (1)$$

provide information relevant to irreversible magnetization changes. The differentiation eliminates the purely reversible components of the switching. Non-zero ρ therefore correspond to components of the magnetization whose reversal is irreversible. The FORC distributions for the graded anisotropy free layer show two primary features of irreversibility (labeled as A and B in Figure 3b). The horizontal ridge noted by Line 1 in Figure 3b corresponds to the precipitous and irreversible drop in magnetization when reverse domains are nucleated. The vertical negative/positive pair of peaks noted by Line 2 in Figure 3b indicates irreversible domain annihilation as negative saturation is approached. The region between Lines 1 and 2 has no peaks but has non-zero ρ. This implies gradual but irreversible changes in the magnetization, which enable the broad range of remanent domain states in the free layer that are necessary to realize field-tunable properties. The feature indicated by Line 3 in Figure 3b suggests abrupt and highly coherent switching of the fixed layer for $H_R \approx -1.4$ kOe. The FORC distribution is essentially featureless between areas A and B because the reversal of the free and fixed layers occurs in distinct field ranges, consistent with the well-defined antiparallel state seen in both the major magnetic hysteresis loop and MR data, Figure 1.

2.4.2. Magnetic Force Microscopy

The tunability of the free layer domain structure by H_R is readily measured by magnetic force microscopy (MFM). The images shown in **Figure 4**a–f were measured at remanence

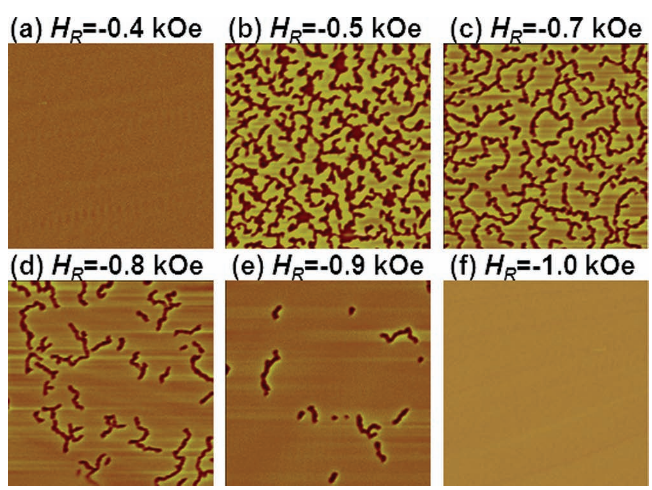

Figure 4. a–f) 20 µm × 20 µm MFM images for H_R = –0.4, –0.5, –0.7, –0.8, –0.9, and –1.0 kOe show the evolution from the parallel to antiparallel states progressing by nucleation and expansion of reversed domains. Dark (bright) domains correspond up (down) domains. The images were taken in zero field following the field protocol used for the resistance measurements.

after applying steps (a) and (b) of the FORC measurement protocol. These data show that the free layer reverses via labyrinth domain nucleation, propagation, and domain annihilation, consistent with the FORC analysis. As the magnitude of H_R increases, the total area of the down (bright) domains increases at the expense of the up (dark) domains. Thus, the field magnitude is essentially recorded as the relative populations of the up and down domains in the free layer. Since these domains are vertically correlated through the free layer,[16,21] and the fixed layer domain state remains uniform for the relevant H_R, the information can be read out as the remanent resistance, mediated by the GMR of the PSV.

In addition to serving as a multistate memory element, the PSVs we report here have potential to act as a memristor.[22] Spintronics-based memristors have been demonstrated with domain wall motion in a free layer induced by spin transfer torques.[23,24] Our PSV devices can be fabricated near a current carrying wire whose Oersted field acts as the means to tune the domain configuration in the free layer. This wire can be connected to a patterned PSV to form a two-terminal device whose resistance depends on the applied current. Additionally, current driven domain wall motion itself[24] could be used to tune the ratio of up/down domains and therefore the remanent resistance.

3. Conclusions

In conclusion, we have demonstrated that PSVs whose free and fixed layers have perpendicular magnetic anisotropy have a virtually continuous range of resistance states that are written by the application of a magnetic field that partially reverses the free layer magnetization. This information is stored in the remanent domain state of the free layer. The state is read simply as the resistance of the spin valve. Thus, these structures have great potential for applications such as field-tunable resistance trimming devices, memristive devices, or magnetic analog memories with a continuous number of states per memory cell, thereby allowing much higher information storage.

4. Experimental Section

The major magnetic hysteresis loop and the family of FORCs were measured with a MicroMag Model 2900 AGM from Princeton Measurements Corporation with the field applied along the surface normal. The MR was measured using a standard home-made four-point dc measurement set-up. The MFM images were captured at zero field using a VEECO Dimension 3100 Atomic Force Microscope with magnetic tips, after first saturating the sample by a 3 kOe magnetic field applied along the film normal followed by applying each H_R.

Acknowledgements

Support from The Swedish Foundation for Strategic Research (SSF), The Swedish Research Council (VR), the Göran Gustafsson Foundation is gratefully acknowledged. J.Å. is a Royal Swedish Academy of Sciences Research Fellow supported by a grant from the Knut and Alice Wallenberg Foundation. The authors thank Dr. Valentina Bonanni for technical support with the four point dc measurement set-up at Royal Institute of Technology (KTH). Work at USF was supported by the NSF.

Received: August 14, 2012
Published online: November 5, 2012

[1] D. D. Tang, Y.-J. Lee, *Magnetic Memory*, Cambridge University Press, New York **2010**.
[2] X. Kou, X. Fan, R. K. Dumas, Q. Lu, Y. Zhang, H. Zhu, X. Zhang, K. Liu, J. Q. Xiao, *Adv. Mater.* **2011**, *23*, 1393.
[3] W. Lim, X. Liu, K. Dziatkowski, Z. Ge, S. Shen, J. Furdyna, M. Dobrowolska, *Phys. Rev. B* **2006**, *74*, 045303.
[4] S. Lee, D. Y. Shin, S. J. Chung, X. Liu, J. K. Furdyna, *Appl. Phys. Lett.* **2007**, *90*, 152113.
[5] Z. Wang, Y. Nakamura, *J. Appl. Phys.* **1996**, *79*, 6639.
[6] M. M. Hassoun, W. C. Black, B. Das, K. A. Wong, *IEEE Trans. Magn.* **1999**, *35*, 2829.
[7] Y. K. Zheng, Y. H. Wu, Z. B. Guo, G. C. Han, K. B. Li, J. J. Qiu, H. Xie, P. Luo, *IEEE Trans. Magn.* **2002**, *38*, 2850.
[8] M. Matczak, P. Kuświk, B. Szymański, M. Urbaniak, M. Schmidt, J. Aleksiejew, F. Stobiecki, A. Ehresmann, *Appl. Phys. Lett.* **2012**, *100*, 162402.
[9] W.-C. Jeong, B.-I. Lee, S.-K. Joo, *J. Appl. Phys.* **1999**, *85*, 4782.
[10] R. Law, R. Sbiaa, T. Liew, T. Chong, *J. Appl. Phys.* **2009**, *105*, 103911.
[11] H. Cramman, D. S. Eastwood, J. A. King, D. Atkinson, *IEEE Trans. Nanotechnol.* **2012**, *11*, 63.
[12] T. Klein, K. Schlage, E. Buchholz, U. Marx, E. Burkel, R. Röhlsberger, *New J. Phys.* **2007**, *9*, 312.
[13] F. J. A. den Broeder, E. Janssen, A. Mud, J. M. Kerkhof, *J. Magn. Magn. Mater.* **1993**, *126*, 563.
[14] M. T. Johnson, J. J. de Vries, N. W. E. McGee, J. aan de Stegge, *Phys. Rev. Lett.* **1992**, *69*, 3575.
[15] G. H. O. Daalderop, P. J. Kelly, F. J. A. D. Broeder, *Phys. Rev. Lett.* **1992**, *68*, 5.
[16] B. J. Kirby, J. E. Davies, K. Liu, S. M. Watson, G. T. Zimanyi, R. D. Shull, P. A. Kienzle, J. A. Borchers, *Phys. Rev. B* **2010**, *81*, 100405(R).
[17] C. R. Pike, A. P. Roberts, K. L. Verosub, *J. Appl. Phys.* **1999**, *85*, 6660.
[18] R. K. Dumas, K. Liu, C. P. Li, I. V. Roshchin, I. K. Schuller, *Appl. Phys. Lett.* **2007**, *91*, 202501.
[19] R. K. Dumas, C. P. Li, I. V. Roshchin, I. K. Schuller, K. Liu, *Phys. Rev. B* **2007**, *75*, 134405.
[20] J. E. Davies, O. Hellwig, E. E. Fullerton, J. S. Jiang, S. D. Bader, K. Liu, G. T. Zimányi, *Appl. Phy. Lett.* **2005**, *86*, 262503.
[21] J. E. Davies, O. Hellwig, E. E. Fullerton, G. Denbeaux, J. B. Kortright, K. Liu, *Phys. Rev. B* **2004**, *70*, 224434.
[22] L. Chua, *Appl. Phys. A* **2011**, *102*, 765.
[23] X. Wang, Y. Chen, H. Xi, H. Li, D. Dimitrov, *IEEE Electron Device Lett.* **2009**, *30*, 294.
[24] A. Chanthbouala, R. Matsumoto, J. Grollier, V. Cros, A. Anane, A. Fert, A. V. Khvalkovskiy, K. A. Zvezdin, K. Nishimura, Y. Nagamine, H. Maehara, K. Tsunekawa, A. Fukushima, S. Yuasa, *Nat. Phys.* **2011**, *7*, 626.